A Final Report to

IBM

on

"Removing Contaminants from Wafers
using Focused Acoustic Waves"

December, 1991.

UM-MEAM-91-18

by

Giles J. Brereton

Assistant Professor

Dept. of Mechanical Engineering and Applied Mechanics

Bradford A. Bruno

Dept. of Mechanical Engineering and Applied Mechanics

The University of Michigan

Ann Arbor, MI 48109

Lorraine G. Olson

Associate Professor

Dept. of Mechanical Engineering

University of Nebraska, Lincoln

eng1
UHR0449

Table of Contents

Report Description

SUMMARY

The experimental study of the interaction between gigahertz-frequency focused acoustic waves and contaminant micron-scale particles on surfaces was successfully completed during this final phase of the project. Using real-time video observation through a microscope, the response of various particle-surface systems to focused acoustic excitation was documented. By varying the duty cycle of acoustic excitation, the mean acoustic energy density in a beam at a surface was controlled in a systematic manner such that: *i*) when exposed to high acoustic energy densities for short durations, weakly attached micron-scale particles can be manipulated selectively about their point of contact with the surface; and *ii*) under continuous exposure to high acoustic energy levels, micron particles which had been adhered to the surface may be displaced large distances normal to the acoustic axis. While the principal means of energizing particles at a surface is thought to be a linear acoustic effect, the mechanism of removal is clearly shown to be driven by a nonlinear secondary effect in which the radial component of radiation pressure causes particle displacement normal to the acoustic axis. Video recordings of particle removal events attest to the importance of this secondary effect which had previously been thought to be insignificant. These results demonstrate the feasibility of the focused acoustic wave as a tool for cleaning contaminated surfaces when used in combination with a simple forced convection system.

In the companion computational studies of the removal of submicron contaminants from wafers using focused acoustic waves over the past three years, our most productive numerical work has involved the simulation of the linear wave-particle-wafer interactions. This work has resulted in greatly improved numerical techniques for treating the complex three-dimensional problem of oblique incidence of acoustic waves on spheres at surfaces.

I. INTRODUCTION

During this final phase of the project, the optical and acoustic systems were refined and implemented in real-time particle removal studies. It was found that particles could be manipulated remotely by the acoustic transducer for excitation over short durations, or removed (though frequently reattaching within 50 microns) under continuous remote acoustic excitation. These findings have been described in an earlier report and companion video tape.[1] In the course of these studies, the importance of secondary acoustic effects to particle motion at surface immediately became apparent. Analyses of the expected behavior of secondary motions led to the identification of the radial gradient in radiation pressure as playing a key role in determining the removal trajectories of displaced particles, consistent with the video observations.[1] While the choice of an acoustic excitation frequency in the gigahertz range was originally based on a hypothesis from linear acoustic theory that one might induce a resonant linear effect if particles were excited at wavelengths commensurate with their diameter, it became apparent in the course of these investigations that the real benefits of using focused acoustic waves at these frequencies were the extremely narrow beam waists which resulted in very high localized power densities, large radial gradients in radiation pressure, and pronounced streaming motions. Each of these effects appears to play a key role in making selective removal of micron particles from surfaces by focused acoustic waves an effective means of cleaning silicon wafers. They are described in the following sections. Computational progress towards efficient solution of the three-dimension interactions between spheres at surfaces and oblique plane waves is also described.

II. BACKGROUND

The existing literature on particle removal from surfaces, and on the adhesive forces between micron-sized particles and surfaces, includes a body of information on physical models describing the pertinent forces, and a number of recent applied studies which concern themselves with the practical issues of particle removal. It is widely believed that the primary means of adhesion of micron and sub-micron particles to surfaces is through Van der Waal's forces, following the proposals of London[2] and Lifschitz[3]. In the idealized case of a sphere (of diameter d) at a distance of closest approach h from a flat surface of the same material, the attractive force has been modeled as:

$$F_A = \frac{Ad}{3h^2} \qquad \text{for } h << 10^{-4} \text{ mm, and}$$

$$F_A = \frac{Bd}{3h^3} \qquad \text{for } h > 10^{-4} \text{ mm}$$

where A and B are treated as constants for the respective materials. The constant A is usually known as the Hamaker constant of the material. While estimates of the constants are available for a range of materials, the distance of closest approach between the particle and the surface is typically unknown, and would depend on surface roughness, particle shape, and the thickness of any gas film adsorbed at these surfaces. In any particle-surface system, it would typically vary from one particle to another, so that a statistical distribution would probably be a more informative measure. Estimates of typical distances of closest approach vary between $h/d \simeq 0.001$ for smooth surfaces with minimal adsorbtion, to $h/d \simeq 0.1$ in the case of rough surfaces.[4]

If mechanical techniques are sought to remove particles from surfaces, it is useful to compare the estimated surface-attractive force with the weight of the particle. This adhesive force-to-weight ratio gives an order-of-magnitude estimate of the number of g's of acceleration which might be necessary to displace such a particle from its position on a surface. If the distance of closest approach is taken as a given proportion of the particle diameter, the adhesive force-to-weight ratio is proportional to either d^{-4} or d^{-5} depending on which model is employed.

For the case of a spherical silica particle on a flat surface in a vacuum, the constants A and B take the approximate values of 10^{-12} erg and 10^{-19} erg cm respectively;[5] according to physical modeling, the adhesive force-to-weight ratio varies as shown in the table below.

Closest Approach (h/d)	10^{-3}	10^{-2}	10^{-1}	1
Diameter d (mm)				
0.01	8×10^{2}	8×10^{-2}	8×10^{-5}	8×10^{-8}
0.001	8×10^{6}	8×10^{4}	8×10^{0}	8×10^{-3}
0.0001	8×10^{10}	8×10^{8}	8×10^{6}	8×10^{2}

Table 1.

From this table, it is clear that a range of plausible distances of closest approach corresponds to variations of many orders of magnitude in estimates of F_A. For the case of particles of a micron in diameter, these models indicate that if the distance of closest approach is described by $h/d \sim 10^{-1}$ or $h/d \sim 10^{-2}$ then it might be possible to provide the required number of g's of acceleration by mechanical means. However, these models indicate that it may be unlikely that particles of 0.1 microns

could be dislodged by inertial techniques which could be applied practically, since the required accelerations would be so great. This contention remains open to question and may be addressed in continuations of the existing study.

Recently, the problem of removing particles from surfaces has been targeted at particles of the micron and sub-micron scale, with emphasis on identification and removal of selected particles which would interfere with device performance. In the approach described in this report, focused acoustic waves at frequencies of around 1 gigahertz (wavelengths in water of $\sim$ 1 micron, the scale of the particle) are aimed at a chosen particle. This selective approach is necessitated by the tenacity with which sub-micron particles adhere to surfaces (as illustrated in Table 1), with a concomitant need for high localized power densities to effect removal. A finite-element computational study of the forces imparted by small-amplitude gigahertz acoustic plane waves to a sphere attached to a surface was been carried out by Olson[11], who concluded that acoustic excitation at wavelengths of the order of the particle diameter led to the greatest amplitude of surface-normal force on the particle. This result and additional computational results referred to in (V) motivated the experimental study of the problem. The experimental and computational contributions to understanding of particle removal by these means are described in this report.

III. EXPERIMENTAL APPROACH

In order to examine the effectiveness of the focused acoustic wave as a tool for removal of micron particles, an experiment was constructed in which particles of known size could be introduced at a surface and their response to forced acoustic excitation observed. The apparatus necessary for these investigations comprised: *i*) an acoustic transducer and the associated electrical driving circuitry; *ii*) a microscope system which images upon a CID array for both real-time observation and video recording; and *iii*) a translucent slide mounted on traversing stages which acts as the particle-surface system.

i) An acoustic transducer was selected for operation in the gigahertz range in order to provide acoustic waves of wavelength of the order of the dimension of the contaminant particle, when immersed in water. Owing to the pronounced absorption of acoustic waves by water at these frequencies, the focal length of the transducer was 40 microns, with a focused beam waist of approximately 1.2 microns. The particular transducer chosen performed optimally in the 0.9 – 1.3 GHz range. In order to allow variation in the transducer duty cycle, and

so the acoustic power delivered to the beam focus, a gigahertz continuous-wave signal from a function generator was gated to an amplifier which drove the transducer. The gating circuitry was designed using circulators so that return acoustic signals received by the transducer could be monitored during portions of the cycle when the transducer was not emitting sound waves — this feature enabled the acoustic return signal to be used for positioning the beam focus at the surface, as well as for detecting particle presence (in the same fashion as an acoustic microscope operates). A schematic diagram of this circuitry is shown in Fig. 1. Considerable effort was expended to provide the necessary isolation and filtering to allow the circuit to operate with minimal signal reflections while providing optimal switching qualities, as described in detail by Schuck.[12]

ii) The microscope system was designed using standard interchangeable objectives and an eyepiece, which allowed magnifications of 400×, 600× and 800×. The objective was focused, through the back of a glass slide, onto the slide surface on which contaminant particles were present. The eyepiece was positioned to image onto a CID area camera, connected to a monitor and video cassette recorder. Lighting was provided in the form of a focused beam of ultra-violet light projected almost parallel to the slide surface, which allowed ample side-scattering of light from the particles at the slide surface to the microscope system, thereby allowing resolution of particles of the order of a micron in diameter. Calibration of the magnifications achieved by this optical arrangement (shown in Fig. 2) were carried out using standard test gratings which are featured at the introduction to each sequence of footage in the video recording submitted earlier.[1]

iii) The particle-surface system comprised a glass microscope slide, the surface of which was purposefully contaminated with particles of known size and composition. The slide could be translated in three directions by micrometer traversing stages, to allow for selective positioning of individual particles at the focus of the acoustic wave. Particles were typically introduced as a suspension in a milli-molar solution of a surfactant (Triton X-100) in distilled water, which acted as an anti-flocculant. Samples of the suspension were sprayed onto the slide and allowed to dry before mounting the slide on its traversing stage and coupling it to the acoustic transducer with a drop of distilled water, as illustrated in Fig. 3.

Prior to interrogation of the response of individual particles to acoustic excitation, the transducer was positioned so that the focus of the acoustic beam was at the slide surface, thereby concentrating acoustic power over the smallest region possible (estimated as a circle of around 1.2 microns in diameter, when modeled as the first zero of an Airy pattern in acoustic intensity). The beam focus was judged to be at the surface when the surface-reflected acoustic signal reached its peak level, as observed on an oscilloscope display. The axis of the acoustic beam could be determined visually when a few small particles were added to the water drop, since they followed axisymmetric acoustic streaming motions which clearly indicated the axis position.

The response of individual particles to controlled acoustic excitation was studied as follows. The transducer was initially energized for a small fraction ($\sim 1/20$) of a duty cycle of 1 μsec, at a driving frequency of 1 GHz, and positioned over the particle of interest. A pulsed mode of operation was chosen to allow the transducer to be driven at appreciable amplitudes without risk of overheating the device, and to allow monitoring of the reflected acoustic signal between periods of energization. The transducer was then translated back and forth across the particle to see if any response could be observed. The driving frequency was then varied and translation repeated. Finally the fraction of the duty cycle for which the transducer was energized was increased and the translation and frequency scanning processes repeated until the particle under interrogation was removed. In other phases of the study, at given driving frequencies and transducer duty cycles, the transducer was translated continuously over the slide in an effort to determine what fraction of the visible contaminant particle population might be removed. All particle responses were recorded using either standard video or high-speed (Kodak Ektapro Motion Analyzer) video formats according to the time resolution required.

IV. EXPERIMENTAL RESULTS

The experimental results we present follow the same order as the sequence of scenes in the video tape which accompanied an earlier progress report.[1] They illustrate: *i*) the importance of secondary fluid-acoustic wave interactions during high-frequency excitation; *ii*) the ability to selectively manipulate individual micron-scale particles by remote acoustic excitation; and *iii*) systematic displacement (cleaning) of all visible particles from areas scanned by the acoustic transducer.

i) Streaming Motions

It is well known that secondary effects arise through the interaction of finite

amplitude acoustic waves propagating through water at high frequencies. The small density changes are coupled nonlinearly to the varying pressure fields induced by sound waves of finite amplitude. Thus, in a quiescent fluid, the mean pressure fields in regions of finite-amplitude acoustic activity differ from those in regions with acoustic activity infinitesimal in amplitude by a measure known as the radiation pressure (see, for example, Beyer[13]). In the case of a gigahertz acoustic wave focused to a waist of about 1.2 μm at a surface and attenuated at about $\alpha \simeq 600$ cm^{-1}, the gradients in radiation pressure in both the radial and axial directions are appreciable and give rise to pronounced streaming motions. These may be seen clearly in the video footage, in which these motions are marked by small particles which (according to Stokes-flow models) should have negligible slip velocities and so characterize faithfully streamlines of these motions. The Reynolds number of the flow (referenced to the particle diameter or to to the transducer displacement from the surface) is of the order of 10^{-4} or 10^{-2} and so assumptions of Stokes flow are fully justified.

The mean Rayleigh radiation pressure $\langle p_{rad} \rangle$ may be modeled (up to and including terms quadratic in pressure-density variation) as the average of the difference between the momentary Lagrangian pressure p^L and the ambient pressure (p_0). It takes the form:

$$\langle p_{rad} \rangle = \langle p^L - p_0 \rangle \simeq \frac{\langle E \rangle}{2} \left(1 + \frac{B}{2A} \right) \tag{1}$$

where $\langle E \rangle$ is the mean acoustic energy density and A and B are the thermodynamic properties $\rho_0 \left(\frac{\partial p}{\partial \rho} \right)_0$ and $\rho_0^2 \left(\frac{\partial^2 p}{\partial \rho^2} \right)_0$ respectively, where $B/A \simeq 5$ for water at 20°C.[13] The dependence on mean acoustic energy density may be demonstrated by increasing the fraction of the duty cycle for which the transducer is energized, causing almost instantaneous acceleration of the marker particles to follow more vigorous streaming motion. When the excitation waveform is turned off, the flow abruptly returns to its quiescent state, wherein the marker particles follow weak motions driven by minor boundary effects.

ii) **Particle Manipulation**

When relatively small fractions of the duty cycles are used to deliver acoustic power to the focus ($\langle E \rangle \simeq 200$ N/m^2 for 1/20 of a cycle, over a circle of diameter 1.2 μm), it is possible to selectively manipulate individual particles about their point of contact with the surface through remote translation of

the acoustic transducer. In a sequence of video scenes on the tape submitted to IBM earlier,[1] the susceptibility of diamond particles (of 2 to 8 microns in size) to external acoustic excitation is demonstrated clearly. The motion of the single particle adjacent to the beam focus is a rotational one in which it realigns itself to present the most streamlined shape towards the axis of the acoustic beam. While it might be thought that drag forces exerted by streaming motions might account for this motion, order of magnitude estimates indicate that these forces are several orders of magnitude smaller than Van der Waal's attractive forces acting on micron scale particles. Moreover, the strong localization of this effect is in contradiction to the more global nature of streaming motions, the observed magnitudes and distributions of which were in good agreement with numerical solutions of this flow.[14] Rather this motion is driven by the imbalance in the momentary radiation pressure forces around the selected particle as the transducer is translated, consistent with the notion of the most stable configuration of bodies in pressure fields corresponding to the orientation which is most streamlined with respect to fluid motion driven by the pressure field. A schematic diagram illustrating remote particle manipulation in this manner is shown in Fig. 4. When acoustic energy is delivered in the same manner to particles which are more weakly attached to the surface, they are abruptly displaced along the surface, normal to the acoustic axis, as evidenced on the video tape which accompanied an earlier progress report.[1]

The observation that an acoustic beam normal to a surface causes particle displacement *along* the surface is instrumental in identifying the principal mechanisms of particle removal through focused acoustic excitation. It clearly cannot be a purely linear acoustic effect, since the linear interaction of a plane wave with a particle at a surface results (ideally) only in surface-normal forces. Moreover, for excitation at gigahertz frequencies, the period of oscillation is not nearly sufficient for micron particles to escape the region of attraction of Van der Waal's forces. The only effects known to us which give rise to forces in the plane of the surface are the radial gradient in radiation pressure at the edge of the beam and the traveling waves induced by the acoustic beam which radiate within the material beneath the surface. If the radial gradient in radiation pressure is estimated as $\langle p_{rad} \rangle / D$, where D is the local beam diameter, and used together with (1) to compute the shear force acting on a micron particle of typical density 1200 kg/m^3, the equivalent acceleration required to provide that force on a micron particle is about $5 \times 10^4\ g$. This acceleration is certainly of the right order for particle removal (according to

Table 1), though it was estimated to be about 10^3 times lower in magnitude than the *amplitude* of the surface-normal acceleration due to linear acoustic interaction.[11] These estimates lead us to believe that, while the principal means of momentarily overcoming the surface attractive force is a linear acoustic effect, it is the gradient in radiation pressure which provides the required force normal to the acoustic axis which allows permanent displacement of a particle from its initial position — without the radial force, the particle might merely detach and reattach at the same location on a flat surface, in response to linear forcing, without any hope of permanent removal.

When micron-scale particles were found which could be manipulated at relatively low energy densities, attempts were made to scan through the operational frequency range of the transducer to explore the possibility of finding a resonant frequency for a given particle at a surface. None could be found for any of the particles interrogated within the range of 0.9 to 1.3 GHz. While computational and analytical models of plane wave interaction with spheres at surfaces have indicated that a linear resonant effect might exist for excitation at a wavelength matching the sphere diameter,[11] it seems unlikely that this result could be extended to grossly non-spherical shapes owing to the multiple characteristic length scales available and the numerous different orientations for particle-surface contact (evidenced in the video tape, for diamond particles). However, we did not have the opportunity to interrogate well-characterized spherical particles on surfaces of known flatness and so the notion of resonant linear interaction remains a topic for more detailed investigation.

iii) **Particle Removal**

Efficient particle removal may be achieved by acoustic excitation at the same amplitude used for particle manipulation, but with excitation over a greater part of the duty cycle. When continuous wave excitation is applied to the transducer, with a mean energy density $\langle E \rangle$ of $\simeq$ 200 N/m^2 at the surface, and the transducer is scanned back and forth along the surface, all visible particles in the transducers path were removed, following trajectories normal to the acoustic axis as observed for low-power removal in *ii*). Many of the particles reattach after displacements of some 30 to 50 microns, and so the addition of forced convection and filtration would be required for a practical implementation of such a cleaning device. The examples of particle removal shown on the video tape were for diamond particles of 2 to 4 microns in size, which were dried to the surface using a heat lamp. These particles frequently present their

largest contact areas to flat surfaces during drying processes and can be difficult to remove effectively by conventional techniques. Thus it is particularly impressive that the focused acoustic wave appears to remove these particles with such ease; it therefore appears to offer great promise as a selective technique for the more demanding problem of removing sub-micron particles, and micron particles which deform when in contact with a flat surface!

In the continuous wave transducer operation described above, the power delivered to the surface was estimated to be about 0.3 mWatts over the largest lobe of the Airy acoustic intensity pattern ($\sim$ 1.2 microns in diameter), corresponding to a local power density of about 11 KWatts/cm^2. It is important to note that the only differences between the excitation applied for particle manipulation and particle removal are in the duration of the applied excitation. The amplitudes and so the momentary forces which arise due to the linear acoustic wave–particle interaction are the same. In contrast, the secondary forces are the *mean* outcome of nonlinearly coupled oscillatory effects and so must be applied continuously over a sufficiently long period to free particles from the region over which surface-attractive forces remain influential and allow outward advection by the streaming motions. Otherwise particle removal will not result. These observations reinforce the notion that an understanding of secondary effects is critical to successful applications of acoustics to particle removal.

COMPUTATIONAL RESULTS

In the companion computational studies of the removal of submicron contaminants from wafers using focused acoustic waves over the past three years, our most productive numerical work has involved the simulation of the linear wave-particle-wafer interactions. Originally, we employed a large finite element mesh and a transient analysis to estimate the force on a contaminant particle on the wafer surface. (This approach was described in a conference presentation[15] and a journal article.[11]) Subsequently, we implemented and tested a simplified two-dimensional numerical model which produced results within 6 percent of those obtained originally, yet this simplified model required only one-thousandth the computational effort. (This was described in several presentations [16,17,18] and a journal article.[19]) In the past year, we began employing fourier decomposition techniques to examine the three-dimensional effects of wave incidence angle on particle removal efficiency. (This approach is described in the attached paper draft in Appendix 1.)

Employing Fourier decomposition methods allows us to estimate the three dimensional forces on the sphere due to waves of arbitrary incidence angle by using two computations (per frequency) on two-dimensional domains. This will result in substantial savings of computer time, which will allow us to investigate the angular effects in significantly more detail.

VI. CONCLUSIONS

In the reports on this project and the companion video recording,[1] the utility of the focused acoustic wave as a tool for selective manipulation of removal of micron scale particles has been demonstrated. This study has been particularly effective in conveying the importance to this application of secondary effects which, in analytical and computational treatments of plane wave–sphere–surface interactions, are all too often neglected. While the choice of an acoustic excitation frequency in the gigahertz range was originally based on a hypothesis from linear acoustic theory that one might induce a resonant linear effect if particles were excited at wavelengths commensurate with their diameter, it soon became apparent that the real benefits of using focused acoustic waves at these frequencies were the extremely narrow beam waists which resulted in very high localized power densities, large radial gradients in radiation pressure, and pronounced streaming motions. Each of these effects appears to play a key role in making selective removal of micron particles from surfaces by focused acoustic waves an effective means of cleaning silicon wafers.

In addition, efficient computer codes have been developed for treating the related model problem of spheres attached to surfaces. These codes should prove invaluable in guiding the refinement in performance of future focused acoustic wave devices when improved transducer technology allows longer focal-length devices to be employed for particle removal through interaction with oblique acoustic waves.

While the capabilities of the focused acoustic wave as a cleaning tool have been demonstrated, there remains some development work to be carried out before it could become a production tool. Foremost amongst the development tasks are: *i*) designs for more rugged transducers, which can deliver greater power than those used in this study; and *ii*) development of a companion forced convection system (possibly a low-frequency focused acoustic wave) to guide displaced particles towards a distant filter, instead of allowing them to reattach to the surface. These refinements might create a real opportunity for selective particle removal at both the micron and submicron scales, in the quest for improved techniques for cleaning silicon wafers.

REFERENCES

1. Brereton, G. J. & Bruno, B. A. Progress report to IBM with companion video tape, June 1991.

2. London, F., Z. Physik, **63**, 245 (1930).

3. Lifschitz, E. M., J. Exp. Theor. Phys. USSR, **29**, 94 (1954).

4. Kaiser, R. In *Particles on Surfaces 2*, ed. K. L. Mittal, Plenum, New York (1989).

5. Casimir, H. G. B. & Polder, D., Phys. Rev., **73**, 360 (1948).

6. Tabor, D. J., Colloid Interface Sci., **58**, 2 (1977).

7. Reed, J. In *Particles on Surfaces 2*, ed. K. L. Mittal, Plenum, New York (1989).

8. Menon, V. B., Michaels, L. D., Donovan, R. P. & Ensor, D. S. In *Particles on Surfaces 2*, ed. K. L. Mittal, Plenum, New York (1989).

9. Berg, D. M., Grimsley, T., Hammond, P. & Sorenson, C. T. In *Particles on Surfaces 2*, ed. K. L. Mittal, Plenum, New York (1989).

10. Willard, G. W., J. Acoustical Soc. Amer., **29 (4)**, 669 (1953).

11. Olson, L. G., J. Sound and Vibration, **126**, 387 (1988).

12. Schuck, M. H., M.S. Thesis, Univ. of Michigan (1990).

13. R. T. Beyer, *Nonlinear Acoustics*, Dept. of the Navy (1974).

14. Bruno, B. A., M.S. Thesis, Univ. of Michigan (1992).

15. L. G. Olson. Sphere–spring–semi-infinite solid problem. First World Congress on Computational Mechanics, September 1986, Austin, TX.

16. L. G. Olson. Finite element model of ultrasonic cleaning, *Journal of Sound and Vibration*, **126** (1988), 387-405.

16. L. G. Olson. A simplified finite element model for ultrasonic cleaning, First U.S. National Congress on Computational Mechanics, July 1991, Chicago, IL.

17. L. G. Olson. Discretization errors in infinite domain problems, American Society of Mechanical Engineers Winter Annual Meeting, December 1991, Atlanta, GA. Text version in *Structural Acoustics*, ASME Press, 1991.

18. L. G. Olson. Nontraditional applications of finite element analysis. Presented at:

Memphis State University, Memphis, TN, April 1991.

U niversity of Nebraska, Lincoln, NE, March 1991.

Universite Catholique de Louvain, Louvain-la-Neuve, Belgium, August 1990.

Illinois Institute of Technology, Chicago, IL, June 1990.

University of Utah, Salt Lake City, UT, May 1990.

Pennsylvania State University, College Station, PA, April 1990.

University of Wisconsin, Madison, WI, March 1990.

19. L. G. Olson. A simplified finite element model for ultrasonic cleaning. *Journal of Sound and Vibration*, in press (1991).

FIGURES

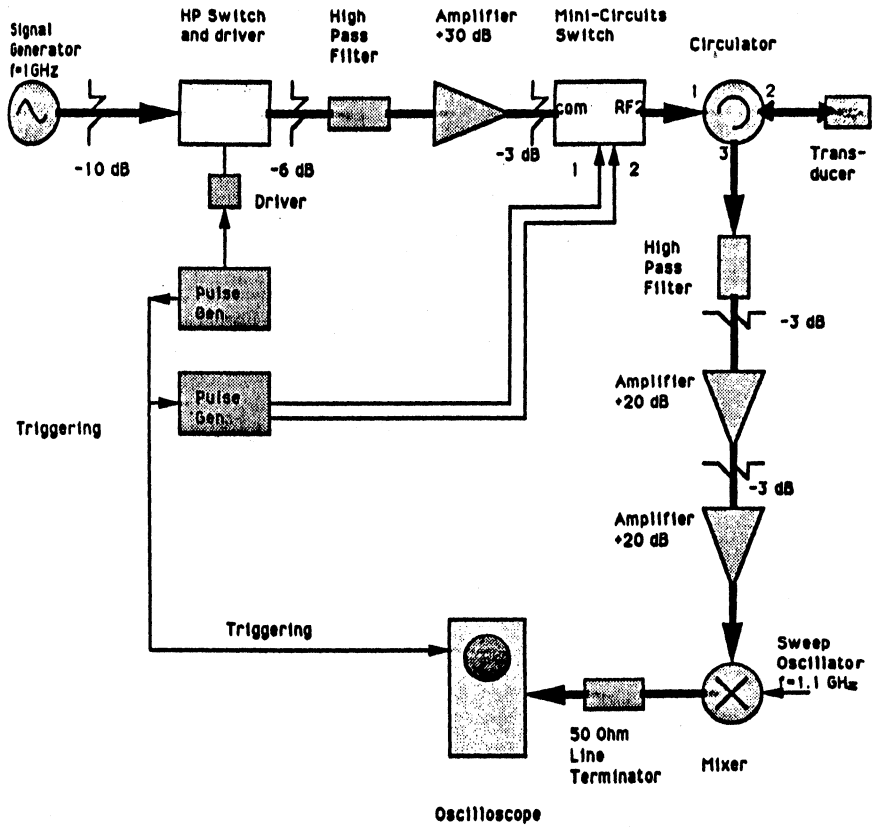

Fig. 1. Circuitry for transducer operation.

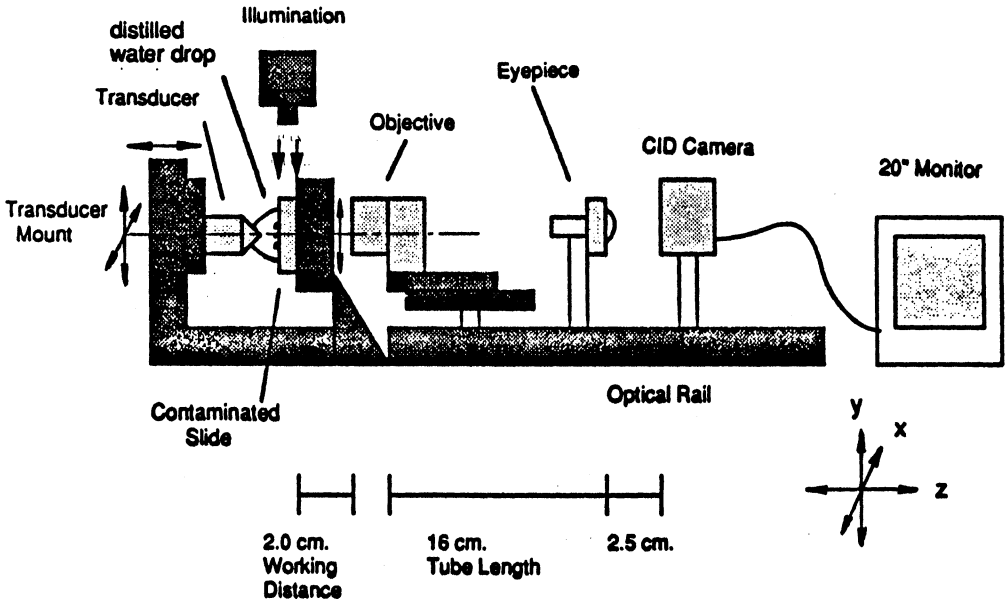

Fig. 2. Microscope system for viewing the particle-surface system.

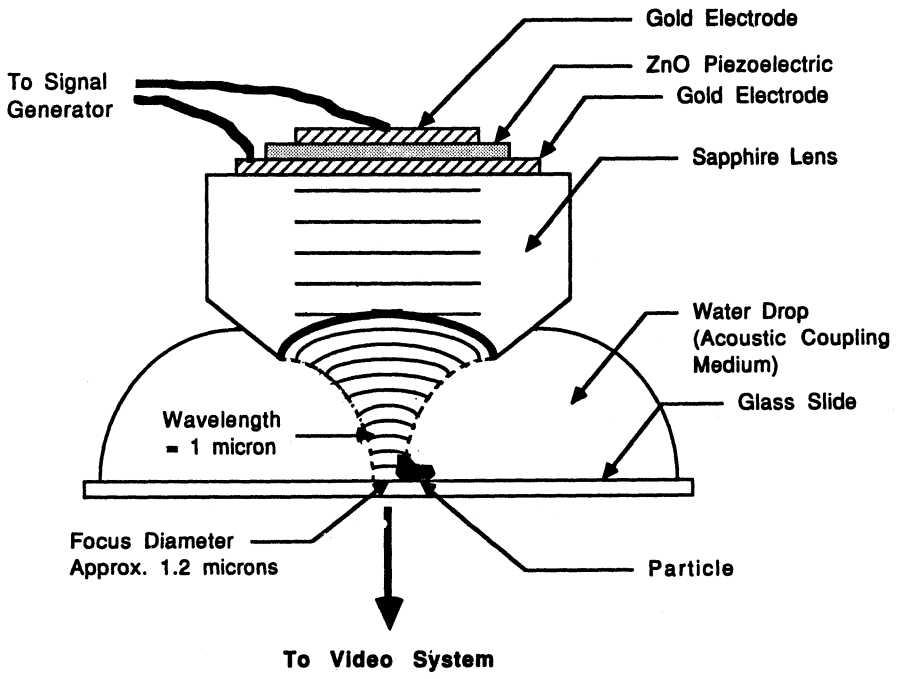

Fig. 3. Transducer coupled to the particle-surface system with a water drop.

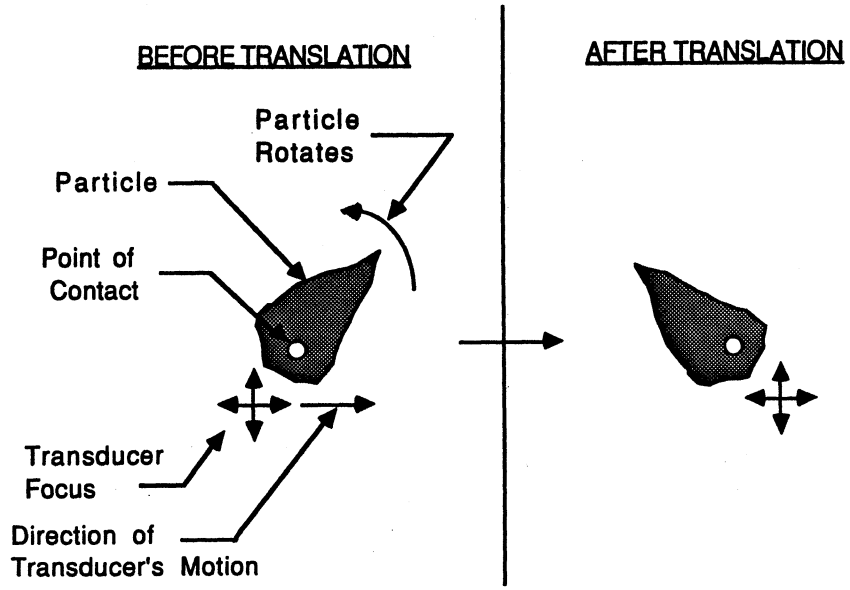

Fig. 4. Particle realignment with the changing radiation pressure field.

1 Introduction

In our previous paper [1], we showed that the solution for the acoustic scattering from a rigid sphere surrounded by water and resting on a semi-infinite half-space of silicon could be approximately modeled as a rigid sphere surrounded by water on a perfectly rigid boundary. In that paper both the geometry and the forcing function (the incident plane wave) were considered to be axisymmetric about the vertical axis. Here we generalize the problem to the case of a plane wave with an off-axis incidence angle. Since the geometry is axisymmetric, but the forcing function is not, we use a Fourier decomposition of the ambient and scattered waves and compute the solution for each fourier component separately.

Fourier decomposition of a non-axisymmetric loading acting on an axisymmetric geometry is a common technique in finite element analysis, and it is well known that it is only computationally efficient when only a few fourier components are required. We show that only two modes (0 and 1) are required if the only information required is the force on the rigid sphere.

Section 2 reviews the governing equations for the general problem, and introduces the Fourier decompostition approach. Section 3 details the expression for the known ambient wave and its Fourier components. The finite element approach to the problem is discussed in Section 4. We are currently in the process of implementing and testing these new procedures, as described in Section 5.

2 Governing Equations

The general system under consideration consists of a rigid 1 μm diameter sphere resting on a rigid plane. The sphere is surrounded by water, which is modelled as an acoustic fluid. The origin of the x, y, z coordinate system is at the intersection of the sphere and the plane, with the y axis vertical. The geometry is axisymmetric about the y axis although the ambient wave is not. Consequently, we will also introduce a cylindrical coordinate system (r, y, θ), with θ measured about the y axis and r the radial coordinate.

We represent the inviscid fluid motion with a velocity potential, ϕ. (We use the sign convention that pressure $p = -\rho\dot{\phi}$, and velocity $\mathbf{u} = \nabla\phi$. ρ is

the fluid density.) The governing equation in the fluid becomes

$$\nabla^2\phi = \frac{1}{c^2}\frac{\partial^2\phi}{\partial t^2} \tag{1}$$

where c is the speed of sound in the fluid and t is time. The boundary conditions are

$$\frac{\partial\phi}{\partial n} = 0 \tag{2}$$

on the rigid surfaces and

$$\phi = \phi^a \tag{3}$$

infinitely far from the sphere. Here n is the unit outward normal from the fluid.

Next we decompose the sound field into the known ambient potential ϕ^a and an unknown scattered potential ϕ^s.

$$\phi = \phi^a + \phi^s$$

The ambient potential satisfies the governing equation in the domain, but does not independently satisfy all of the boundary conditions. The governing equation and boundary condition on the rigid surfaces for the scattered potential become

$$\nabla^2\phi^s = \frac{1}{c^2}\frac{\partial^2\phi^s}{\partial t^2} \tag{4}$$

and

$$\frac{\partial\phi^s}{\partial n} = -\frac{\partial\phi^a}{\partial n}, \tag{5}$$

respectively. Far from the sphere

$$\phi^s = 0. \tag{6}$$

Notice that since the ambient wave is known, the right hand side of equation 5 is given.

In their present form, the governing equations may be used for a transient analysis. As in our previous papers, we will recast the equations in the frequency domain. The ambient wave and the scattered wave may be written as

$$\phi^a = Im\left[\Phi^a e^{i\omega t}\right] \tag{7}$$

and

$$\phi^s = Im\left[\Phi^s e^{i\omega t}\right]. \tag{8}$$

Consequently the governing equations and boundary conditions for the problem become

$$\nabla^2\Phi^s = -\frac{\omega^2}{c^2}\Phi^s, \tag{9}$$

in the domain,

$$\frac{\partial\Phi^s}{\partial n} = -\frac{\partial\Phi^a}{\partial n}, \tag{10}$$

on rigid surfaces, and

$$\Phi^s = 0 \tag{11}$$

far from the sphere. Notice that Φ^s and Φ^a are now complex quantities.

Now let us express the ambient and scattered velocity potentials as a fourier series

$$\Phi = \Phi^s + \Phi^a = \sum_{m=0}^{m=\infty} \left(\Phi^s_m(r,y) + \Phi^a_m(r,y)\right)\cos m\theta$$

where θ is the angle about the y axis. Then we can write the governing equations and boundary conditions for each mode separately.

$$\frac{\partial^2\Phi^s_m}{\partial y^2} + \frac{m^2}{r^2}\Phi^s_m + \frac{\partial^2\Phi^s_m}{\partial r^2} = -\frac{\omega^2}{c^2}\Phi^s \tag{12}$$

in the domain,

$$\frac{\partial\Phi^s_m}{\partial n} = -\frac{\partial\Phi^a_m}{\partial n} \tag{13}$$

on rigid surfaces, and

$$\Phi^s_m = 0 \tag{14}$$

far from the sphere. The modes are decoupled due to the orthogonality of the $\cos m\theta$ terms.

In general, we must compute the results for several modes and sum them in order to get an accurate result for the scattered potential. However, if we seek only the force on the rigid sphere we only need to compute the results for modes 0 and 1.

To understand why only two modes are necessary for the force calculation, consider the expression for the force on the sphere:

$$\mathbf{F} = -\int p\mathbf{n}dS = -\int i\rho\omega\Phi\mathbf{n}dS$$

The x and y components of the force on the rigid sphere become

$$F_x = -\int i\rho\omega\Phi(a,y)\sqrt{2ay-y^2}\cos\theta d\theta dy$$

and

$$F_y = -\int i\rho\omega\Phi(a,y)(y-a)d\theta dy$$

The z component of the force on the sphere is zero. After performing the θ integration, the force expressions reduce to

$$F_x = -\Pi\int i\rho\omega(\Phi_1^s(a,y)+\Phi_1^a(a,y))\sqrt{2ay-y^2}dy$$

and

$$F_y = -2\Pi\int i\rho\omega(\Phi_0^s(a,y)+\Phi_0^a(a,y))(y-a)dy$$

The x-direction force is orthogonal to all but the first mode. The y-direction force is orthogonal to all but the zeroth (axisymmetric) mode.

3 Characterization of the Ambient Wave

The ambient wave is given by

$$\Phi^a = 2\cos\left(\frac{\omega y}{c}\cos\alpha\right)e^{i(\frac{\omega}{c}\sin\alpha)r\cos\theta} \tag{15}$$

On the sphere, we have

$$\Phi^a = 2\cos\left(\frac{\omega y}{c}\cos\alpha\right)e^{i(\frac{\omega}{c}\sin\alpha)\sqrt{2ay-y^2}\cos\theta} \tag{16}$$

and

$$\frac{\partial\Phi^a}{\partial n} = [A(y)\cos\theta + B(y)]e^{i(\frac{\omega}{c}\sin\alpha)\sqrt{2ay-y^2}\cos\theta} \tag{17}$$

where

$$A(y) = i2\frac{\omega}{c}\sin\alpha\cos\left(\frac{\omega y}{c}\cos\alpha\right)\frac{\sqrt{2ay-y^2}}{a} \tag{18}$$

$$B(y) = -2\frac{\omega}{c}\cos\alpha \sin(\frac{\omega y}{c}\cos\alpha)\frac{y-a}{a} \tag{19}$$

In order to calculate the forces on the sphere, we must evaluate the fourier components for the ambient field. Because of the $\cos\theta$ term in the exponential in equations 16 and 17, it is difficult to evaluate the terms exactly. Consequently we use a series representation to approximate the exponential, and integrate the series in the θ direction. After some significant calculation, we find the following approximate results:

$$\frac{\partial \Phi_0^a}{\partial n} = I_1 A(y) + I_0 B(y) \tag{20}$$

where

$$I_0 \approx \frac{1}{2}(2 - \frac{\beta}{2} + \frac{\beta^2}{32}) \tag{21}$$

$$I_1 \approx \frac{i}{2}(1 - \frac{\beta^3}{8} + \frac{\beta^5}{192}) \tag{22}$$

and

$$\beta = \frac{\omega}{c}\sin\alpha\sqrt{2ay - y^2} \tag{23}$$

$$\frac{\partial \Phi_1^a}{\partial n} = I_2 A(y) + I_1 B(y) \tag{24}$$

where

$$I_2 \approx \frac{1}{2}(1 - \frac{3}{8}\beta^2 + \frac{1}{192}\beta^4) \tag{25}$$

$$\Phi_0^a = \cos(\frac{\omega y}{c}\cos\alpha)[2 - \frac{\beta}{2} + \frac{\beta^2}{32}] \tag{26}$$

$$\Phi_1^a = 2i\cos(\frac{\omega y}{c}\cos\alpha)[1 - \frac{\beta^3}{8} + \frac{\beta^5}{192}] \tag{27}$$

The absolute error in each of these components is less than 10^{-3}.

4 Finite Element Discretization

We use the 2-D fluid mesh from our previous paper [1] to model the problem. The sphere and the plane are completely rigid. Near the sphere, the fluid is modeled with bilinear acoustic elements. The infinite elements satisfy the far-field boundary condition $\Phi^s = 0$ in an approximate sense.

The governing matrix finite element equations for the problem become:

$$[\mathbf{K}_{ff} + \mathbf{K}_{inf} + i\omega\mathbf{C}_{inf} - \omega^2\mathbf{M}_{ff}]\Phi_m^s = \mathbf{F}_f \tag{28}$$

Here $\mathbf{K}_{ff}$ and $\mathbf{M}_{ff}$ are the added mass and compressibility matrices for the acoustic fluid, and $\mathbf{K}_{inf}$ and $\mathbf{C}_{inf}$ are the approximate added mass and damping matrices for the infinite elements. The forcing function for the system is given by

$$\mathbf{F}_f = \int \rho \frac{\partial \Phi_m^a}{\partial n} \mathbf{h}\, ds \tag{29}$$

where $\mathbf{h}^T = [\ h_1\ h_2\ \ldots\ ]$, h_i is the shape function for node i, and the integration is over the planar (r,y) surface of the sphere.

The only difference between the standard axisymmetric form for $\mathbf{K}$, $\mathbf{C}$, and $\mathbf{M}$ and their form for the fourier decomposition occurs in the $\mathbf{K}_{ff}$ matrix. It is given by

$$\mathbf{K}_{ff} = \int \rho \mathbf{D}^T \mathbf{D} r\, dr\, dy \tag{30}$$

with

$$\mathbf{D} = \begin{bmatrix} \frac{\partial h_1}{\partial y} & \frac{\partial h_2}{\partial y} & \ldots \\ \frac{\partial h_1}{\partial r} & \frac{\partial h_2}{\partial r} & \ldots \\ \frac{m}{r} h_1 & \frac{m}{r} h_2 & \ldots \end{bmatrix} \tag{31}$$

The last row in $\mathbf{D}$ is not required for axisymmetric analysis (m=0).

5 Simulation Results

We are currently in the process of testing the finite element formulation just described. We will examine the forces on the sphere for various wave incidence angles and a range of frequencies near 1 GHz.

References

[1] L. G. Olson, A simplified finite element model of ultrasonic cleaning. *Journal of Sound and Vibration*, in press (1991).